BIOCHEMISTRY
including biophysical chemistry & molecular biology

ARTICLE

pubs.acs.org/biochemistry

Heparin Binds 8 kDa Gelsolin Cross-β-Sheet Oligomers and Accelerates Amyloidogenesis by Hastening Fibril Extension

James P. Solomon, Steve Bourgault, Evan T. Powers, and Jeffery W. Kelly*

Departments of Chemistry and Molecular and Experimental Medicine and Skaggs Institute for Chemical Biology, The Scripps Research Institute, 10550 North Torrey Pines Road, La Jolla, California 92037, United States

Supporting Information

ABSTRACT: Glycosaminoglycans (GAGs) are highly sulfated linear polysaccharides prevalent in the extracellular matrix, and they associate with virtually all amyloid deposits in vivo. GAGs accelerate the aggregation of many amyloidogenic peptides in vitro, but little mechanistic evidence is available to explain why. Herein, spectroscopic methods demonstrate that GAGs do not affect the secondary structure of the monomeric 8 kDa amyloidogenic fragment of human plasma gelsolin. Moreover, monomerized 8 kDa gelsolin does not bind to heparin under physiological conditions. In contrast, 8 kDa gelsolin cross-β-sheet oligomers and amyloid fibrils bind strongly to heparin, apparently because of electrostatic interactions between the negatively charged polysaccharide and a positively charged region of the 8 kDa gelsolin assemblies. Our observations are consistent with a scaffolding mechanism whereby cross-β-sheet oligomers, upon formation, bind to GAGs, accelerating the fibril extension phase of amyloidogenesis, possibly by concentrating and orienting the oligomers to more efficiently form amyloid fibrils. Notably, heparin decreases the 8 kDa gelsolin concentration necessary for amyloid fibril formation, likely a consequence of fibril stabilization through heparin binding. Because GAG overexpression, which is common in amyloidosis, may represent a strategy for minimizing cross-β-sheet oligomer toxicity by transforming them into amyloid fibrils, the mechanism described herein for GAG-mediated acceleration of 8 kDa gelsolin amyloidogenesis provides a starting point for therapeutic strategy development. The addition of GAG mimetics, small molecule sulfonates shown to reduce the amyloid load in animal models of amyloidosis, to a heparin-accelerated 8 kDa gelsolin aggregation reaction mixture neither significantly alters the rate of amyloidogenesis nor prevents oligomers from binding to GAGs, calling into question their commonly accepted mechanism.

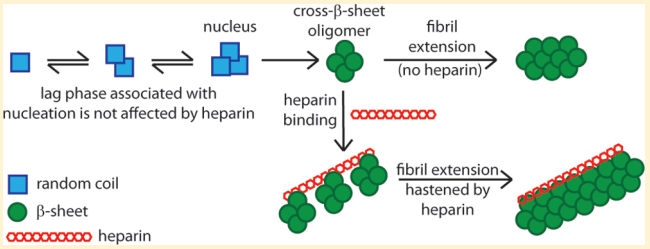

Glycosaminoglycans (GAGs) are linear sulfated polysaccharides that are prevalent in the extracellular matrix and consist of repeating disaccharide units.[1] GAGs are associated with virtually all extracellular amyloid deposits, formed from one of 30 different human amyloidogenic proteins linked to distinct amyloid diseases,[2] including immunoglobulin light chains, transthyretin, amyloid β (Aβ), and the serum amyloid A protein.[3] Thus, GAGs appear to play a vital role in amyloid deposition in mammals, by a mechanism that remains unclear.[4,5] The hypothesis that the tissue-selective distribution of different GAGs creates distinct extracellular environments with differential abilities to accelerate amyloidogenesis potentially explains why different amyloidogenic proteins lead to the degeneration of specific tissues and why different mutants of the same protein can cause proteotoxicity in distinct tissues.

It has been proposed that cells upregulate the formation of sulfated GAGs to reduce organismal proteotoxicity.[6] In support of such a mechanism, it has been previously demonstrated that exogenous addition of various GAGs protects against Aβ_{42} proteotoxicity,[7] Dutch mutant Aβ_{40} proteotoxicity,[8] and possibly degeneration by the human prion protein,[9] although this latter effect is not always seen.[10] One explanation for the protective effect of GAGs is that they stabilize amyloid fibrils and shield the surface of amyloid from the remainder of the proteome, preventing aberrant protein recruitment, thus rendering the amyloid less proteotoxic. Herein, we show that GAGs can transform proteotoxic oligomers into less toxic amyloid fibrils, representing another possible mechanism of protection.

Biophysical experiments conclusively demonstrate that the addition of GAGs to human amyloidogenic proteins accelerates their amyloidogenesis in vitro. These proteins include Aβ,[11] β_2-microglobulin,[12,13] transthyretin,[14] and the amyloidogenic fragments of gelsolin.[15] Although detailed and convincing mechanistic studies to explain the acceleration of amyloidogenesis are scarce, numerous mechanisms have been proposed to explain how GAGs accelerate amyloidogenesis. Herein, we endeavor to understand the mechanism of GAG-accelerated amyloidogenesis of the 8 kDa fragment of human plasma gelsolin, the clinically most important fragment in gelsolin amyloid disease.[16]

Gelsolin has six domains, each of which can bind a Ca^{2+} ion.[17] There are two splice variants of gelsolin: an 81 kDa intracellular variant that is responsible for remodeling the actin cytoskeleton

Received: November 29, 2010
Revised: February 23, 2011
Published: February 24, 2011

by facilitating actin polymerization or fragmentation and an 83 kDa version secreted into the plasma that is responsible for scavenging actin fibrils released from injured tissue into the blood, thereby preventing increases in blood viscosity.[18] Plasma gelsolin also likely has other functions.[19,20] Several types of cells secrete gelsolin into the blood, although muscles seem to be the major source of secreted gelsolin.[21]

A G654 to A or T DNA point mutation changes an aspartate at position 187 to either an asparagine (D187N) or tyrosine (D187Y), respectively, upon translation. These mutations eliminate the position 187 carboxylate side chain calcium binding ligand, dramatically lowering the Ca^{2+} binding affinity of the second domain of plasma gelsolin, compromising its stability.[22−24] Without the stabilization afforded by Ca^{2+} binding, domain 2 can sample the unfolded state as it passes through the Golgi on its way to the cell surface, the unfolded population being susceptible to cleavage by furin in the *trans* Golgi, producing a secreted C-terminal 68 kDa gelsolin fragment (C68).[21−26] The secreted C68 fragment is then cleaved again, apparently in the extracellular matrix, to generate 8 and 5 kDa amyloidogenic fragments, with the former being the main component of gelsolin amyloid fibrils in humans[16] and the amyloidogenic fragment studied herein. While it is clear that membrane type 1 matrix metalloprotease (MT1-MMP) can perform this cleavage step in cultured cells,[27] other proteases in the extracellular matrix may also contribute. The formation of the 8 and 5 kDa amyloidogenic peptides appears to cause familial amyloidosis of Finnish type (FAF) through systemic amyloid deposition in the basement membrane of the skin,[28] blood vessel walls,[29] eyes,[30] and peripheral nervous system.[31]

We have recently created a murine model of FAF featuring a muscle-specific promoter to drive D187N gelsolin synthesis and secretion.[32] This model recapitulates the aberrant endoproteolytic cascade and the aging-associated extracellular amyloid deposition of human FAF. Amyloidogenesis is observed only in tissues synthesizing human D187N gelsolin, despite the presence of the 68 kDa cleavage product in blood. As in humans, gelsolin fragment amyloidogenesis and accumulation are closely associated with GAGs in the extracellular matrix.[32] In fact, GAGs are substantially upregulated in this mouse model as the amyloid disease progresses, suggesting that GAG overexpression may be linked to pathology or protection from the process of amyloidogenesis.

The gelsolin amyloidogenic peptides have recently been established to aggregate by a nucleated polymerization mechanism,[33] and their aggregation rate is known to be profoundly accelerated by addition of heparin.[15] Herein, we demonstrate that heparin does not alter the intrinsically disordered structure of the monomeric 8 kDa amyloidogenic fragment of human plasma gelsolin. We also show that the binding of monomerized 8 kDa gelsolin to heparin cannot be detected at neutral pH, even at the concentration of 50 μM utilized in the NMR experiments. Complementary experiments also fail to detect a binding interaction. We provide strong evidence to support the hypothesis that cross-β-sheet oligomers and amyloid fibrils bind to heparin, apparently because of an electrostatic interaction between the positively charged regions of the 8 kDa gelsolin aggregates and the negatively charged, sulfated polysaccharide. Our observations suggest that heparin binds to 8 kDa gelsolin oligomers, hastening the fibril extension phase of the nucleated polymerization reaction, possibly by binding to postnucleation cross-β-sheet oligomers, facilitating quaternary structural conversion into larger aggregates. Notably, the presence of heparin is able to decrease the concentration of 8 kDa gelsolin necessary for the accumulation of thioflavin T (TfT)-positive aggregates, likely by fibril binding and stabilization. We demonstrate that GAG mimetics, including those used in amyloid disease clinical trials, do not slow the rate of GAG-mediated 8 kDa gelsolin amyloidogenesis in vitro, nor do they seem to affect the solubility of the gelsolin amyloid fibrils.

MATERIALS AND METHODS

Preparation of the 8 kDa Amyloidogenic Fragment of Gelsolin. The 8 kDa amyloidogenic fragment of gelsolin (corresponding to amino acids 173−242) was prepared as previously described.[33,34]

Preparation of the Monomerized 8 kDa Amyloidogenic Fragment of Gelsolin. The 8 kDa amyloidogenic fragment was monomerized by dissolving 1−4 mg of lyophilized 8 kDa gelsolin (amount dependent on the desired final concentration) in 500 μL of 8 M guanidinium hydrochloride (GdnHCl) and 50 mM sodium phosphate (NaP_i) (pH 7.5). The solution was sonicated in a water bath sonicator for at least 2 h. It was then buffer exchanged using a 20 mL Superdex 30 gel filtration column that had been equilibrated with 50 mM NaP_i, 100 mM NaCl, and 0.02% NaN_3 (pH 7.2) (unless otherwise specified). The monomerized peptide peak, free of chaotrope, eluted after ~9 mL and was collected and used immediately in subsequent experiments.

Circular Dichroism (CD) Experiments. The monomeric 8 kDa amyloidogenic fragment prepared in 10 mM KP_i and 50 mM K_2SO_4 (pH 7.0), as this buffer allowed for better measurements at wavelengths of <205 nm, was diluted to a concentration of 20 μM, either in the absence or in the presence of 30 μg/mL heparin (purchased from Calbiochem, heparin sodium salt from porcine intestinal mucosa). For the quiescent experiments, the gelsolin was allowed to sit at room temperature, while for the agitation experiments, it was mixed using overhead rotation (24 rpm) at 37 °C. Periodically, 200 μL was removed, and a far-UV CD spectrum was recorded using an AVIV model 202SF CD spectrometer. Quartz cells with 0.1 or 0.2 cm path lengths were used. The wavelength step size used was 1 nm with an averaging time of 2 s for each wavelength. The buffer and buffer with heparin controls were subtracted from the 8 kDa gelsolin and 8 kDa gelsolin with heparin data, respectively; their contribution to mean residue ellipticity (MRE) was <2% of that of gelsolin (Figure 1 of the Supporting Information).

Fluorescence Anisotropy Studies. Heparin was fluorescently labeled according to a procedure described by Glabe et al.[35] Briefly, the reducing end of heparin was activated by the addition of 15 mg of cyanogen bromide (CNBr) to a solution of 30 mg of heparin in 1 mL of water (pH 11). Once the CNBr had completely dissolved, the solution was allowed to incubate at room temperature for 10 min. The reaction mixture was then desalted using a G-25 column that had been preequilibrated in 0.2 M sodium borate (pH 8.0) for buffer exchange and removal of excess CNBr. Fluoresceinamine (3 mg) was immediately added to the eluate, and the reaction mixture was incubated overnight at room temperature. To remove unreacted fluoresceinamine, the reaction mixture was again run over a G-25 desalting column that had been preequilibrated in 50 mM NaP_i, 100 mM NaCl, and 0.02% NaN_3 (pH 6.8). The final concentration of the fluoresceinated heparin was 3 mg/mL.

For anisotropy studies, the monomerized 8 kDa amyloidogenic fragment of gelsolin was diluted to a concentration of 20 μM and agitated via overhead rotation (24 rpm) at 37 °C. Periodically, 90 μL of the sample was removed and added to

10 μL of a 1:10 dilution of the fluoresceinated heparin solution and the fluorescence anisotropy examined in an AVIV fluorimeter (excitation at 485 nm, emission at 515 nm). Each anisotropy reading was taken at least five times. A TfT fluorescence reading was taken at the same time as the anisotropy assessment to determine the aggregation state. For the fluorescence readings, 20 μL of the 8 kDa gelsolin solution was added to 80 μL of 25 μM TfT (final concentration of 20 μM) in a quartz cuvette and evaluated in a Cary Eclipse fluorescence spectrophotometer (excitation at 440 nm, emission at 485 nm).

Heparin Affinity Chromatography. The monomerized 8 kDa amyloidogenic fragment of gelsolin was diluted to a concentration of 20 μM and agitated via overhead rotation at 37 °C. Periodically, 300 μL of the sample was removed and injected at a rate of 1 mL/min onto a 1.5 mL column of Heparin HyperD Affinity resin (Pall Corp.) that had been preequilibrated with 50 mM NaP_i, 100 mM NaCl, and 0.02% NaN_3 (pH 7.2). After the column had been rinsed with at least 5 column volumes of buffer, a gradient up to 4 M NaCl over 5 column volumes was used for elution. After the gradient, the column was rinsed with 2 column volumes of 7.2 M GdnHCl in 50 mM NaP_i (pH 7.5). Once again, a TfT fluorescence reading was taken at the same time as the affinity chromatography assessment to determine the aggregation state.

One-Dimensional Proton NMR Experiments. For all experiments, heparin was diluted such that the disaccharide subunit concentration was 50 μM in a solution consisting of 90% 50 mM NaPi, 100 mM NaCl, and 0.02% NaN_3 (pH 7.4) and 10% of D_2O. For the heparin and monomerized 8 kDa gelsolin sample, 8 kDa gelsolin was monomerized as described above and added to a final concentration of 50 μM. For the heparin and 8 kDa gelsolin fibril sample, 50 μM freshly monomerized 8 kDa gelsolin was added to the heparin solution and rotated at 24 rpm at 37 °C for 3 h to make amyloid fibrils, the presence of which was confirmed by TfT fluorescence. A 500 MHz ^{1}H NMR spectrum (8K scans with water suppression) was recorded using an Avance 501 NMR spectrometer.

Gel Mobility Shift Assay. Monomerized 8 kDa gelsolin was diluted to a concentration of 24 μM in 50 mM NaP_i, 100 mM NaCl, and 0.02% NaN_3 (pH 7.2) and rotated at 37 °C for 2 h (24 rpm) to form amyloid fibrils, the presence of which was verified by TfT fluorescence. A freshly monomerized 8 kDa gelsolin solution was allowed to incubate on ice for 2 h and did not exhibit TfT fluorescence. Fluoresceinated heparin (60 μg/mL) was then added to each of the solutions (affording a 1:6 heparin:8 kDa gelsolin fragment molar ratio), and the mixtures were incubated for 30 min at 25 °C. As a positive control, fluoresceinated heparin was mixed with 300 μg/mL protamine sulfate, a known binder of heparin. Glycerol (2 μL) was then added to 10 μL of each of the solutions, and these were loaded into the wells of a 1.2% (w/v) agarose gel in 90 mM Tris, 90 mM borate, and 2 mM EDTA (pH 8.3). Electrophoresis was conducted at 100 V for 1 h in the same buffer. The fluoresceinated heparin was visualized by UV fluorescence.

Plate Reader Aggregation Assay. The 8 kDa amyloidogenic fragments were monomerized as described above and diluted to the desired concentrations in 50 mM NaP_i, 100 mM NaCl, and 0.02% NaN_3 (pH 7.2). For experiments involving GAGs or GAG mimetics, the oligosaccharides were dissolved in the same buffer and added to the solution to achieve the reported concentration. For examination of TfT fluorescence, the solution also contained a final TfT concentration of 20 μM.

All components were mixed together in an Eppendorf tube, and 97 μL of each solution was transferred to a well of a 96-well microplate in triplicate (black plate with a clear bottom, Corning Inc., Corning, NY). The plate was sealed with an airtight lid to minimize evaporation and then placed in a Gemini SpectraMax EM fluorescence plate reader (Molecular Devices, Sunnyvale, CA). For the duration of the experiment, the plate was incubated at 37 °C. Every 10 min, the plate was shaken for 5 s and the fluorescence measured from the bottom of the plate (excitation at 440 nm, emission at 485 nm). Each reading was the mean of 30 individual scans.

Using Wolfram Mathematica 8, the data set from each individual well was fit to the Finke−Watzky model of nucleation according to the equation

$$F_t = F_f + (F_i - F_f) \times \frac{\frac{k_1}{k_2} + [A]_0}{1 + \frac{k_1}{k_2[A]_0}\exp(k_1 + k_2[A]_0)t} \quad (1)$$

where F_t is the fluorescence at time t, F_f is the fluorescence of the completely aggregated sample (the end of the assay), F_i is the fluorescence of the freshly monomerized sample (the beginning of the assay), and $[A]_0$ represents the concentration of 8 kDa gelsolin used in the experiment. By fitting the data using this equation, we could determine the t_{50}, or time required to reach 50% fibril formation. Notably, the constant k_1 is proportional to the inverse of the lag phase time, and the constant k_2 is proportional to the slope of the curve during the fibril extension phase, affording quantitative information about these phases of the 8 kDa gelsolin aggregation reaction.[36]

Atomic Force Microscopy (AFM). The 8 kDa amyloidogenic fragment of gelsolin was pretreated to afford monomer as described above, diluted to a concentration of 24 μM, either in the absence or in the presence of 10 μg/mL heparin, and agitated via overhead rotation (24 rpm) at 37 °C to form amyloid fibrils. Periodically, aliquots of the reaction mixture were removed and examined by TfT fluorescence as described above and by AFM to discern aggregate morphology. For the AFM sample, 2 μL of the 8 kDa amyloidogenesis reaction mixture was diluted into 18 μL of buffer, and the resulting solution was adsorbed to a surface of freshly cleaved mica for 1 min. The liquid was then wicked off the surface of the mica with filter paper. Salt and unbound material were removed when the sample was washed three times with 20 μL of distilled water that was immediately wicked off the surface of the mica with filter paper. AFM images were recorded using a Digital Instruments multimode scanning probe microscope with a Nanoscope IIIa controller and force modulation etched silicon probes.

Analytical Size Exclusion Chromatography Coupled to Light Scattering. The 8 kDa amyloidogenic fragment of gelsolin was monomerized as described above, diluted to a concentration of 24 μM, and agitated via overhead rotation (24 rpm) at 37 °C. Experiments were performed using a 20 mL Superdex 75 analytical gel filtration column with in-line 0.1 μm filters or a 2 mL Superdex 75 analytical gel filtration column without any filters. For the larger, 20 mL column, periodically, 400 μL of the 8 kDa amyloidogenesis reaction mixture was removed and loaded into a sample loop for loading onto the column. For the smaller, 2 mL column, periodically, 75 μL of the sample was removed, 75 μL of buffer was added for dilution, and the solution was spun at 15000*g* for 2 min to pellet any large aggregates. The

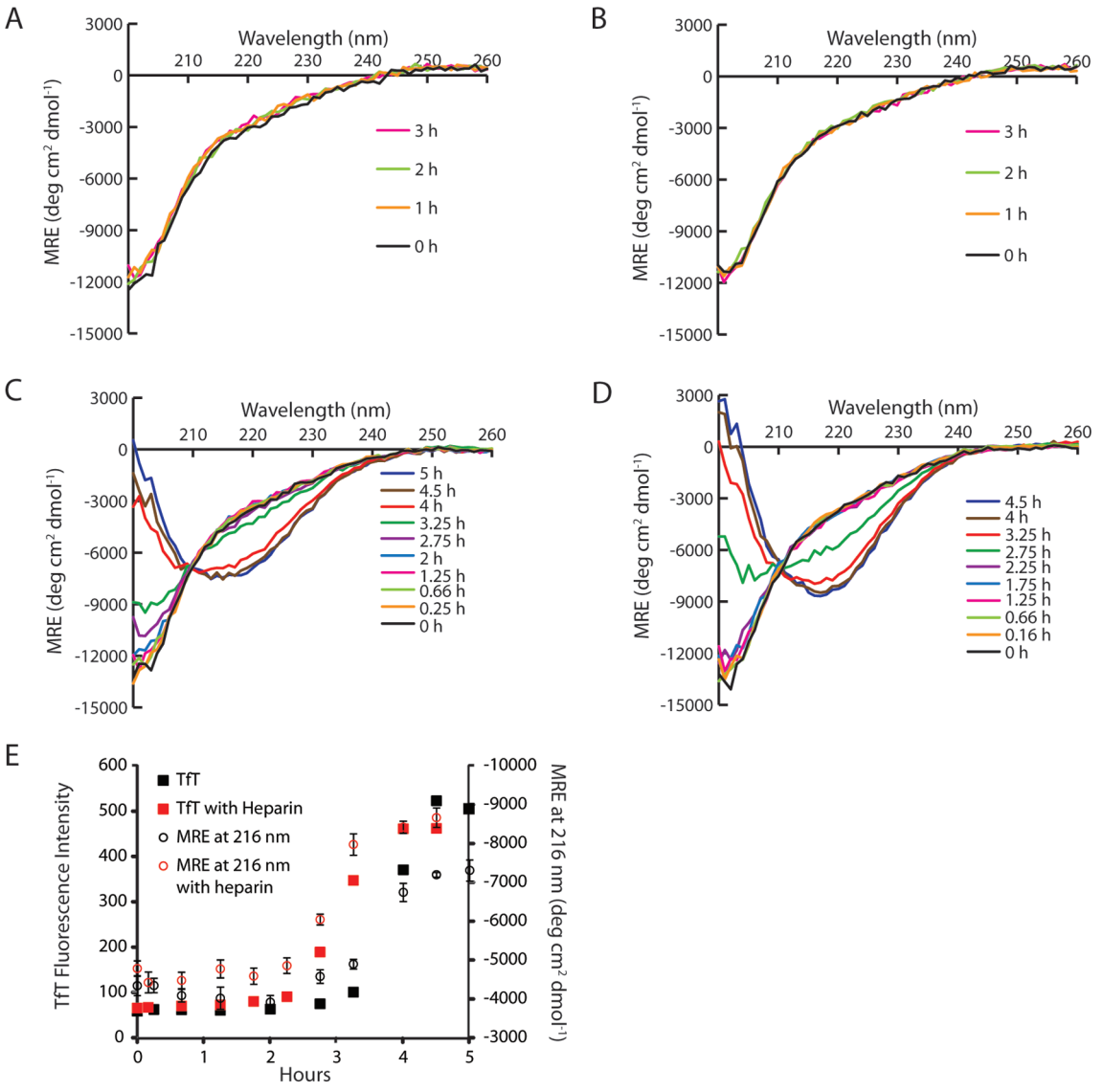

Figure 1. Effect of heparin on the secondary and quaternary structure of the 8 kDa gelsolin fragment. The 8 kDa gelsolin fragment (20 μM) was incubated quiescently at 37 °C in the absence (A) or presence (B) of 30 μg/mL heparin and was periodically examined by far-UV CD (cell path length of 0.1 cm). No changes were observed over the course of 3 h. (C) When 8 kDa gelsolin (20 μM) was agitated via overhead rotation (24 rpm) at 37 °C, the secondary structure changed from random coil to cross-β-sheet quaternary structures (cell path length of 0.2 cm). (D) The addition of heparin (30 μg/mL) decreased the time required for the formation of cross-β-sheet quaternary structures (cell path length of 0.2 cm). (E) The increase in the level of cross-β-sheet quaternary structure, as measured by mean residue ellipticity (MRE) at 216 nm (○, with error bars representing the standard deviation in the measurement), occurs at the same time as the increase in TfT fluorescence (■, with error bars representing the standard deviation in the measurement smaller than the size of the points), in the absence (black) and presence (red) of heparin, suggesting that the 8 kDa fragment of gelsolin does not alter its random coil secondary structure until it begins to aggregate and bind TfT.

supernatant was then loaded into a 25 μL sample loop and loaded onto the column. In each case, the mobile phase of the Superdex 75 column consisted of 50 mM NaP_i, 100 mM NaCl, and 0.02% NaN_3 (pH 7.2). The column eluate was then directly injected into a Dawn EOS light scattering photometer (Wyatt Technology, Santa Barbara, CA) that was connected to the FPLC system for measurements of 90° static light scattering as well as dynamic light scattering. In both cases, a TfT fluorescence reading was taken at the same time as the analytical size exclusion chromatograph to determine the aggregation state, as described above.

Fitting to Nucleated Polymerization with a Competing Off-Pathway Oligomerization Model. Data from a plate reader aggregation assay in triplicate wells of a 96-well plate were arithmetically averaged and plotted as the TfT fluorescence intensity versus time. The baseline was subtracted, and the data up to either 25 or 50% of the TfT fluorescence at completion of the amyloidogenesis reaction were fit to a second-order polynomial using Microsoft Excel. The residuals were calculated by subtraction of the best fit second-order polynomial from the experimental data.

RESULTS

Addition of Heparin Does Not Change the Intrinsically Disordered Structure of 8 kDa Gelsolin. Far-UV circular dichroism (CD) spectroscopy was employed to determine whether

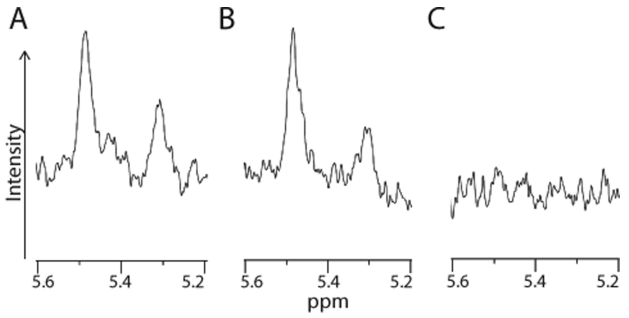

Figure 2. 1D 500 MHz ^{1}H NMR spectra with water suppression. (A) The proton NMR spectrum of heparin (50 μM disaccharide subunit concentration) has two characteristic resonances at 5.3 and 5.5 ppm that do not overlap with any ^{1}H NMR resonances from the 8 kDa fragment of gelsolin (50 μM) in solution. (B) These resonances do not change intensity or chemical shift when an equimolar concentration of monomerized 8 kDa gelsolin is added. (C) When a solution of 50 μM heparin and 50 μM monomerized 8 kDa gelsolin is agitated via overhead rotation at 37 °C for 3 h, so that amyloid fibrils are formed, the characteristic heparin resonances are no longer observed.

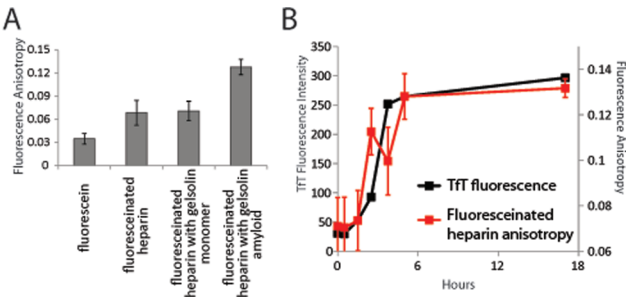

Figure 3. Heparin was labeled with fluorescein to probe its binding to various forms of 8 kDa gelsolin utilizing anisotropy. (A) The fluorescence anisotropy after 8 kDa gelsolin aggregation for 5 h, once amyloid fibrils had been formed (bar at the far right), was significantly greater than the anisotropy at the beginning of the experiment when all of the 8 kDa gelsolin was monomeric (second bar from the right). Fluoresceinated heparin (second bar from the left) and fluorescein alone (far left bar) are included as controls. (B) The increase in anisotropy paralleled the formation of 8 kDa gelsolin (20 μM) amyloid fibrils discerned by TfT binding-associated fluorescence, demonstrating binding of the amyloid fibrils to fluoresceinated heparin.

the presence of heparin affects the intrinsically disordered structural ensemble of the monomerized 8 kDa amyloidogenic fragment of gelsolin. When freshly monomerized 8 kDa gelsolin (20 μM) was incubated quiescently without heparin for 3 h, no discernible change in the far-UV CD spectrum was observed (Figure 1A). A strictly analogous quiescent sample with heparin added at a concentration of 30 μg/mL (molecular mass of 13.5−15 kDa) exhibited an unaltered CD spectrum as well (Figure 1B), indicating no discernible change in the intrinsically disordered structural ensemble of 8 kDa gelsolin. When 8 kDa gelsolin (20 μM) in the absence of heparin was agitated via overhead rotation (24 rpm), a procedure we previously employed to produce amyloid fibrils from this intrinsically disordered protein,[33] aggregation was observed, as reflected by the conversion of a random coil to a cross-β-sheet quaternary structure over the course of 5 h (Figure 1C). In a strictly analogous sample with heparin added [30 μg/mL (Figure 1D)], the conversion to a cross-β-sheet quaternary structure occurred on a slightly accelerated time scale (cf. 0.66 h CD spectrum of Figure 1C,D).

To probe whether this slightly hastened conversion to a cross-β-sheet quaternary structure was due to an effect of heparin on the intrinsically disordered ensemble of conformers of monomeric 8 kDa gelsolin or to an accelerated postnucleation step, the kinetics of the increase in β-sheet character, as measured by mean residue ellipticity at 216 nm was compared to the kinetics of amyloid fibril formation, as measured by TfT fluorescence (Figure 1E; excitation at 440 nm, emission at 485 nm). In the absence and presence of heparin, the increase in the level of β-sheet quaternary structure detected by far-UV CD strictly coincides with the formation of amyloid monitored by TfT fluorescence. The fact that the heparin-accelerated time course of amyloid fibril formation and the heparin-accelerated time course of β-sheet quaternary structure formation are very similar, if not identical (red symbols), provides further evidence that it is unlikely that heparin affects the conformational ensemble of monomerized 8 kDa gelsolin or any prenucleation step.

The 8 kDa Gelsolin Amyloid Fibrils Bind to Heparin, whereas Monomeric 8 kDa Gelsolin Does Not. To further scrutinize the hypothesis that monomeric 8 kDa gelsolin does not bind to heparin, one-dimensional (1D) 500 MHz ^{1}H NMR experiments were performed. The ^{1}H NMR spectrum of polydisperse heparin (13500−15000 Da, at a disaccharide repeat subunit concentration of 50 μM) was recorded, revealing two diagnostic singlet peaks at 5.31 and 5.48 ppm that are in a region of the spectrum in which there are no resonances from 8 kDa gelsolin (Figure 2A and Figure 2A of the Supporting Information). Upon addition of monomerized 8 kDa gelsolin (50 μM), there was no change in the chemical shifts or intensity of the heparin peaks at 5.31 and 5.48 ppm, which would be expected to change if monomeric 8 kDa gelsolin was binding to heparin (Figure 2B and Figure 2B of the Supporting Information). In striking contrast, when heparin was mixed with 8 kDa gelsolin and agitated via overhead rotation (24 rpm and 37 °C) to form amyloid fibrils, the peaks at 5.31 and 5.48 ppm were not observed (Figure 2C and Figure 2C of the Supporting Information). The formation of 8 kDa gelsolin cross-β-sheet amyloid fibrils in this rotated sample was confirmed by TfT fluorescence. Thus, it appears that an interaction between soluble heparin and 8 kDa gelsolin cross-β-sheet structures dramatically increased the T_2 spin−spin relaxation time of heparin, leading to substantial heparin peak broadening.

To further probe the interaction between heparin and the 8 kDa fragment of gelsolin, we performed fluorescence anisotropy experiments with fluoresceinated heparin. Fluoresceinated heparin was able to accelerate the aggregation of the 8 kDa amyloidogenic fragment of gelsolin to the same extent as unlabeled heparin in a TfT fluorescence plate reader-based aggregation assay (Figure 3 of the Supporting Information). Fluoresceinated heparin exhibited a significantly higher anisotropy than fluorescein by itself (Figure 3A).

The anisotropy of fluoresceinated heparin in the presence of monomerized 8 kDa gelsolin was not significantly different from the anisotropy of fluoresceinated heparin in buffer (in Figure 3A, cf. the height of the second and third bars), although only a small increase in anisotropy was anticipated if the fluoresceinated heparin (13.5−15 kDa) were to bind the 8 kDa gelsolin monomers in 1:1 stoichiometry, as the molecular mass of the complex would be 23 kDa. When monomerized 8 kDa gelsolin (20 μM) was agitated via overhead rotation (24 rpm) at 37 °C to allow amyloidogenesis, the anisotropy was significantly higher (Figure 3A, far right

bar). These results were confirmed using a 96-well fluorescence polarization plate reader assay (Figure 4 of the Supporting Information). The increase in fluoresceinated heparin anisotropy paralleled the formation of amyloid fibrils, as reflected by TfT fluorescence (Figure 3B). Because the heparin anisotropy increased as the cross-β-sheet oligomers and fibrils were being formed, we can conclude that the postnucleation cross-β-sheet oligomers and fibrils bind to fluoresceinated heparin.

To confirm the binding of 8 kDa gelsolin amyloid fibrils to heparin, aliquots (400 μL) of an 8 kDa gelsolin (24 μM) amyloidogenesis reaction mixture were removed at various time points and loaded onto a 2 mL heparin affinity column. Heparin-binding 8 kDa gelsolin structures were eluted with a gradient of up to 4 M NaCl before the column was cleaned with a denaturing solution [7.2 M GdnHCl and 50 mM NaP_i (pH 7.5)] (Figure 5 of the Supporting Information). Freshly monomerized 8 kDa gelsolin did not bind to the resin, as all of it flowed through before the gradient was started (Figure 5B of the Supporting Information). After rotation for 2.5 h, when TfT-positive fibrils and/or cross-β-sheet oligomers were present in the sample, the flow-through peak was dramatically decreased in intensity (Figure 5C of the Supporting Information). Integration reveals that the flow-through peak of the 8 kDa gelsolin fibrillar sample was 22% of the area of the flow-through peak of the monomerized 8 kDa gelsolin sample, indicating substantial binding. No additional peaks were observed when a gradient of up to 4 M NaCl was applied, suggesting very strong binding between the 8 kDa gelsolin oligomers and/or amyloid fibrils and the immobilized heparin (Figure 5C of the Supporting Information). However, when the column was cleaned with 7.2 M guanidinium chloride, an additional peak was observed corresponding to the 8 kDa gelsolin fragment comprising cross-β-sheet quaternary structures. This observation is consistent with the expectation that 8 kDa gelsolin cross-β-sheet structures and fibrils bind very tightly to heparin and the only means of eluting 8 kDa gelsolin aggregates is to utilize chaotrope solutions that partially or fully denature the amyloid fibrils.

Because it is conceivable that the cross-β-sheet oligomers and amyloid bind nonspecifically to the Sepharose core of the heparin affinity resin, the same experiment was performed using a Superdex 75 Sepharose-based size exclusion column as a control. With this resin, both freshly monomerized 8 kDa and the 8 kDa gelsolin oligomers and/or fibrils after being mixed for 2.5 h were able to flow through the column (panels E and F of Figure 5 of the Supporting Information, respectively). Integration showed that the Superdex 75 flow-through peaks of the monomerized and fibrillar 8 kDa gelsolin samples were 95 and 93%, respectively, of the area of the monomerized 8 kDa gelsolin heparin affinity column flow-through peak, demonstrating a lack of binding. No additional peaks were observed when 4 M NaCl or 7.2 M guanidine was applied. The volume required for elution of the 8 kDa gelsolin monomer was not significantly different from that of the 8 kDa gelsolin fibrils because the volume of the size exclusion column (2 mL) was small compared to the volume of the samples examined (400 μL).

Finally, to further demonstrate that 8 kDa gelsolin amyloid fibrils can interact with heparin, while the 8 kDa gelsolin monomer cannot, a gel mobility shift assay was performed. In this assay, free, unbound fluoresceinated heparin migrates rapidly toward the anode unless it forms a complex with gelsolin structures, which alters the migration by both increasing the size and altering the overall charge of the complex, allowing

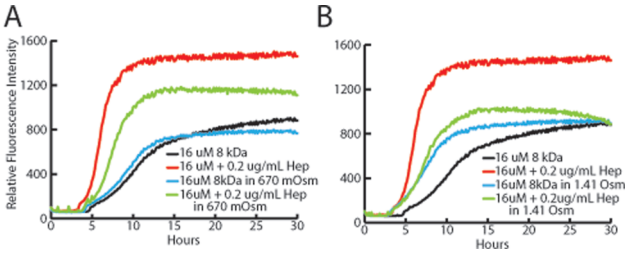

Figure 4. Effect of salt concentration on heparin-dependent acceleration of 8 kDa gelsolin amyloidogenesis. Various volumes of a 2 M NaCl solution were added to the amyloidogenesis reaction mixtures to yield an osmolarity of 670 mOsm (A) or 1.41 Osm (B). The data from each individual well were fit to the Finke–Watzky model (eq 1), and constants k_1 and k_2, as well as the t_{50} values listed in Table 1, depict the arithmetic average of data from triplicate wells. Collectively, these data demonstrate that increasing the ionic strength dramatically decreases the rate of heparin acceleration of 8 kDa gelsolin amyloidogenesis.

separation and subsequent visualization by fluorescence.[37] The addition of monomerized 8 kDa gelsolin (24 μM) to fluoresceinated heparin (50 μg/mL) did not appreciably change the mobility of fluoresceinated heparin (in Figure 6 of the Supporting Information, cf. lanes 1 and 2). The addition of 8 kDa gelsolin amyloid fibrils, however, had a substantial effect on the mobility of a fraction of fluoresceinated heparin. The fluoresceinated heparin remaining at the top of the gel was retained by 8 kDa gelsolin amyloid fibril binding (in Figure 6 of the Supporting Information, see lane 3). As a positive control, positively charged protamine sulfate, a known binder of heparin, was also examined, which prevented the migration of fluoresceinated heparin (in Figure 6 of the Supporting Information, see lane 4).

Importance of Electrostatic Interactions for the Conversion of Quaternary Structure. To test the hypothesis that the 8 kDa gelsolin oligomer–amyloid fibril heparin interaction is predominantly an electrostatic interaction, the salt concentration of the buffer was varied in a plate reader aggregation assay. When the osmolarity of the aggregation reaction buffer is increased from the standard physiological conditions of 300 mOsm to 670 mOsm by addition of NaCl, the rate at which 8 kDa gelsolin aggregates in the absence of heparin is slightly increased (in Figure 4A, cf. blue vs black traces), while the rate at which 8 kDa gelsolin aggregates in the presence of heparin is clearly reduced [in Figure 4A, cf. green (high-salt) vs red (low-salt) traces]. Further increasing the osmolarity of the aggregation reaction buffer to 1410 mOsm almost eliminates heparin acceleration of the 8 kDa gelsolin amyloidogenesis, in that the kinetics of gelsolin aggregation is nearly the same in the absence and presence of heparin (in Figure 4B, cf. green vs blue traces).

Each trace in Figure 4 is the arithmetic average of data from triplicate wells of a representative experiment. We recognize that these types of TfT fluorescence aggregation assays performed in a plate reader can have large variations and thus exhibit reproducibility challenges. However, our rigorous pretreatment method, combined with the inherent biophysical properties of the 8 kDa fragment of gelsolin, renders these experiments reproducible. To demonstrate the low variability in the time courses, data from each individual well from the experiment presented in Figure 4 are shown in Figure 7 of the Supporting Information. In addition, to confirm that the observations made in this experiment are reproducible, we performed the assay a total of three times on

Table 1. Constants k_1 and k_2 and t_{50} Values from Fitting Data from the Plate Reader Aggregation Assays to the Finke−Watsky Model (eq 1)[a]

	k_1 (h^{-1})	k_2 ($\mu M^{-1} h^{-1}$)	t_{50}[b] (h)
	Experiments for Figure 4		
16 μM 8 kDa[c]	$(1.63 \pm 0.09) \times 10^{-2}$	$(1.57 \pm 0.02) \times 10^{-2}$	10.68 ± 0.11
16 μM 8 kDa and 0.2 μg/mL heparin	$(2.27 \pm 0.13) \times 10^{-3}$	$(6.17 \pm 0.16) \times 10^{-2}$	6.15 ± 0.09
16 μM 8 kDa at 670 mOsm	$(5.40 \pm 0.52) \times 10^{-3}$	$(3.14 \pm 0.06) \times 10^{-2}$	8.97 ± 0.09
16 μM 8 kDa at 670 mOsm and 0.2 μg/mL heparin	$(2.00 \pm 0.09) \times 10^{-3}$	$(4.92 \pm 0.13) \times 10^{-2}$	7.58 ± 0.17
16 μM 8 kDa at 1410 mOsm[d]	$(1.15 \pm 0.13) \times 10^{-2}$	$(3.30 \pm 0.01) \times 10^{-2}$	7.17 ± 0.20
16 μM 8 kDa at 1410 mOsm and 0.2 μg/mL heparin	$(5.60 \pm 0.35) \times 10^{-3}$	$(4.06 \pm 0.03) \times 10^{-2}$	7.29 ± 0.14
	Experiments for Figure 5		
16 μM 8 kDa[c]	$(9.29 \pm 0.61) \times 10^{-3}$	$(8.73 \pm 0.14) \times 10^{-3}$	19.04 ± 0.29
16 μM 8 kDa and 1 μg/mL heparin	$(8.38 \pm 0.23) \times 10^{-3}$	$(2.04 \pm 0.06) \times 10^{-2}$	11.08 ± 0.17
16 μM 8 kDa and 1 mM eprodisate	$(7.17 \pm 1.40) \times 10^{-3}$	$(1.08 \pm 0.07) \times 10^{-2}$	18.20 ± 0.49
16 μM 8 kDa, 1 mM eprodisate, and 1 μg/mL heparin	$(8.20 \pm 0.18) \times 10^{-3}$	$(2.10 \pm 0.03) \times 10^{-2}$	10.94 ± 0.14
16 μM 8 kDa and 1 mM homotaurine[d]	$(4.30 \pm 2.28) \times 10^{-3}$	$(1.22 \pm 0.29) \times 10^{-2}$	19.86 ± 1.13
16 μM 8 kDa, 1 mM homotaurine, and 1 μg/mL heparin	$(5.58 \pm 0.53) \times 10^{-3}$	$(2.44 \pm 0.11) \times 10^{-2}$	10.81 ± 0.36

[a] The plots of the fits are shown in Figure 8 of the Supporting Information. The values are average k_1, k_2, and t_{50} values (with standard devations) of two or three individual fits of data to eq 1 from triplicate wells from a representative plate reader aggregation assay. [b] t_{50} was calculated as the time at which the sigmoidal curve reached 50% of the maximal fluorescence. [c] The experiments were performed at different pH values (7.0 for the Figure 4 experiment and 7.2 for the Figure 5 experiment), which accounts for the difference in values for similar experiments. It should be noted, however, that while amyloidogenesis is exquisitely sensitive to reaction conditions, the observations presented and discussed here and in Figures 4 and 5 (that increasing salt concentration reduces the effect of heparin on aggregation rate and that GAG mimetics have no effect on aggregation rate in the presence or absence of heparin) were made in at least three independent experiments. [d] One of the data sets for this condition was poor (see Figure 7 of the Supporting Information), so these values reflect an average of only duplicate wells.

three separate occasions using two different preparations of the 8 kDa fragment of gelsolin. Separate plate reader aggregation assays are difficult to compare because the 8 kDa gelsolin fragment was freshly monomerized in each assay, leading to slight alterations in osmolarity and pH to which the amyloidogenicity time courses of 8 kDa gelsolin are very sensitive.[33] However, the same trends in the data (increasing osmolarity increases the aggregation rate of 8 kDa gelsolin in the absence of heparin while decreasing the aggregation rate in the presence of heparin) were robust and always observed.

The data from each individual well from the representative experiment were also fit to the Finke−Watzky model of nucleation according to eq 1, and the values of k_1 and k_2, along with the calculated t_{50}, are listed in Table 1 (the individual data sets and their best fit curves are shown in Figure 8 of the Supporting Information). Although the Finke−Watzky model probably oversimplifies the mechanism of amyloidogenesis and is primarily a phenomenological model, some quantitative information can be gleaned from fitting the data to this model via eq 1.[36] The k_1 values, theoretically proportional to the inverse of the lag phase of the reaction, are exquisitely sensitive to the data fitting early in the reaction, and these early time points did not always fit well to eq 1 (see Figure 8 of the Supporting Information). Therefore, we cannot make any significant observations about the correlation of k_1 values with lag time. However, we could make some interesting observations about constant k_2, which is proportional to the slope of the curve during the fibril extension phase.[36] Under physiological salt conditions (300 mOsm), the presence of heparin results in k_2 values that are significantly higher than they are in the absence of heparin. As the concentration of salt is increased to 670 mOsm and then to 1410 mOsm, the difference between the k_2 values of the samples with and without heparin decreases. The expected trend was also observed for the calculated t_{50} values. A large and significant difference was observed between the t_{50} of the sample with heparin and that of the sample without heparin at the physiological salt concentration. This difference was decreased with the addition of NaCl to a final concentration of 670 mOsm, and there was no significant difference in t_{50} between the heparin-containing sample and the sample without heparin at 1410 mOsm.

It should also be noted that there is a substantial difference in the amplitude of the TfT fluorescence among some of the samples (Figure 4). The quantum yield of TfT is affected by the polarity and rigidity of its microenvironment, and it has been proposed that TfT interacts with the cross-β-sheet structures of amyloid.[38] Many possibilities exist, however, for the difference in microenvironment reflected by the difference in quantum yield, including fibril structure, bound glycosaminoglycans, etc., and it is difficult to be more specific about these amplitude changes without structural data to guide our hypotheses.

Effect of GAG Mimetics. GAG mimetics, sulfonated small molecules that mimic the sulfated sugars of the extracellular matrix, are hypothesized to ameliorate human amyloidoses by inhibiting the interaction between amyloidogenic peptides and GAGs in the extracellular matrix, thus reducing the extent of GAG-mediated acceleration of amyloid fibril formation.[39−41] If true, the addition of the GAG mimetics eprodisate sodium and homotaurine should slow the heparin-dependent acceleration of the rate of the 8 kDa gelsolin amyloidogenesis reaction as examined by TfT fluorescence, provided the GAG mimetics themselves do not accelerate amyloidogenesis. The GAG mimetics themselves did not alter the rate of 8 kDa gelsolin amyloidogenesis [in Figure 5, cf. orange and green traces in the presence of the mimetics to the trace for gelsolin alone (black)]. Moreover, even at a concentration of 1 mM, much higher than that of heparin (1 μg/mL or 2 μM based on

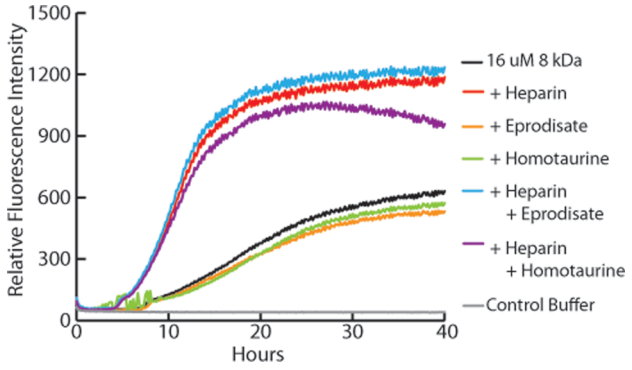

Figure 5. Influence of GAG mimetics eprodisate sodium (1 mM) and homotaurine (1 mM) on the aggregation rate of the amyloidogenic 8 kDa fragment of gelsolin in the absence and presence of 1 μg/mL heparin. The data from each individual well were fit to the Finke−Watzky model (eq 1), and constants k_1 and k_2, as well as the t_{50} values listed in Table 1, are the arithmetic average of data from triplicate wells. Collectively, these data suggest that GAG mimetics have no effect on 8 kDa gelsolin amyloidogenesis.

disaccharide repeats), the GAG mimetics only minimally affected the heparin-dependent acceleration of the rate of 8 kDa gelsolin amyloidogenesis (in Figure 5, cf. red, blue, and purple traces). Again, each trace in Figure 5 is the arithmetic average of data from triplicate wells from a representative experiment, and data from each individual well are shown in Figure 7C of the Supporting Information. To confirm the observations described, this experiment was performed a total of three times on three separate occasions using two different preparations of the 8 kDa fragment of gelsolin, and no significant effect of the GAG mimetics on aggregation kinetics was ever observed.

To confirm the lack of any significant influence of the GAG mimetics on 8 kDa gelsolin amyloidogenesis, the data from individual wells from the representative experiment were again fit to the Finke−Watzky model (eq 1). The values of k_1, k_2, and t_{50} listed in Table 1 (fitted curves shown in Figure 8B of the Supporting Information) reveal that the addition of the GAG mimetics, in the presence or absence of heparin, shows no significant effect on either k_2 or t_{50}. Thus, the GAG mimetics tested were unable to inhibit the interaction of heparin with the amyloidogenic 8 kDa fragment of gelsolin in vitro, consistent with the expectation that the interaction between heparin and gelsolin oligomers is polyvalent. In contrast, the 8 kDa gelsolin aggregation reactions that occurred in the presence of heparin exhibit k_2 values that are significantly higher and t_{50} values significantly lower compared to those of the reactions in the absence of heparin.

Examining the Early Stages of Gelsolin Amyloidogenesis. Analytical size exclusion chromatography coupled with light scattering was employed next to probe the early stages of the 8 kDa gelsolin amyloidogenesis reaction. The 8 kDa gelsolin (24 μM) in 50 mM NaP_i, 100 mM NaCl, and 0.02% NaN_3 (pH 7.2) was mixed via overhead rotation (24 rpm) to form amyloid fibrils. At various time points during the amyloidogenesis reaction, aliquots were removed and loaded onto a Superdex 75 size exclusion column with a mobile phase of the same buffer. Upon elution of 8 kDa gelsolin from the column, the static light scattering at 90° and dynamic light scattering were measured. The TfT fluorescence of the aliquot was also examined to assess the presence of amyloid fibrils or oligomeric cross-β-sheet aggregates.

We first reproduced the experiments previously described by Suk et al.[15] using a 20 mL Superdex 75 column with an in-line 0.1 μm filter. In the absence of heparin, the magnitude of the monomer peak decreases with time, but no oligomers can be observed directly, as they are likely filtered out of the solution before they are able to flow through the column (Figure 9A of the Supporting Information). The decrease in the magnitude of the monomer peak occurs concomitantly with an increase in TfT fluorescence, suggesting the presence of fibrils. In the presence of heparin, however, a significant oligomer peak is observed as soon as TfT-positive oligomers are observed (in Figure 9B of the Supporting Information, cf. absorbance and 90° light scattering traces), in addition to the previously observed decrease in the magnitude of the monomer peak. It should be noted that the 8 kDa gelsolin fragment used in this work corresponds to amino acids 173−242, whereas in the previous work, an 8 kDa gelsolin fragment of amino acids 173−243 was used; however, this change is not expected to change aggregation propensity.[15] In addition, the monomerization procedure is more rigorous in this work, using GdnHCl and size exclusion chromatography to completely remove any oligomers.

An analogous experiment was performed with a slightly altered setup, in that a 2 mL Superdex 75 column without any in-line filters was used instead of the 20 mL Superdex 75 column. In addition, a much smaller sample was injected (see Materials and Methods). In this enhanced experimental paradigm, in the absence of heparin, cross-β-sheet oligomers were observed as soon as the TfT fluorescence began to increase (in Figure 6A, cf. absorbance and 90° light scattering traces), although the mass balance was still poor (<40%), likely because fibrils were retained on top of the column. In the presence of heparin, more cross-β-sheet oligomers were observed (Figure 6B) and the mass balance was better (>80%). Dynamic light scattering reveals that the hydrodynamic radius of the oligomers in the oligomer peak, in the presence and absence of heparin, is between 60 and 80 nm. It should be noted that the light scattering of the oligomers going through the column does not line up exactly with the absorbance peaks and is spread out because the volume of the sample was small compared to the volume of the flow cell. Collectively, these experiments demonstrate that no oligomeric species can be seen by size exclusion chromatography until the solution exhibits TfT fluorescence, an observation that, along with the far-UV CD spectroscopy data presented in Figure 1E, suggests a transition from monomeric random coil 8 kDa gelsolin to cross-β-sheet oligomers without highly populated intermediates.

It is particularly interesting that more oligomers are able to pass through the column in the presence of heparin. A possible explanation is that the cross-β-sheet oligomers and fibrils, once formed, are bound to heparin in the solution, thus inhibiting their lateral association into insoluble material that is retained by the column.[15]

Because heparin appears to "solubilize" the aggregates and prevent them from associating and forming large structures, it was therefore hypothesized that the GAG mimetics such as eprodisate sodium may function in vivo by a similar mechanism, and they were examined in this experimental paradigm. The addition of eprodisate sodium did not increase the solubility of the 8 kDa gelsolin oligomers in the absence of heparin, as roughly the same amount of oligomers is able to pass through the column as without eprodisate (cf. panel C to panel A of Figure 6). The

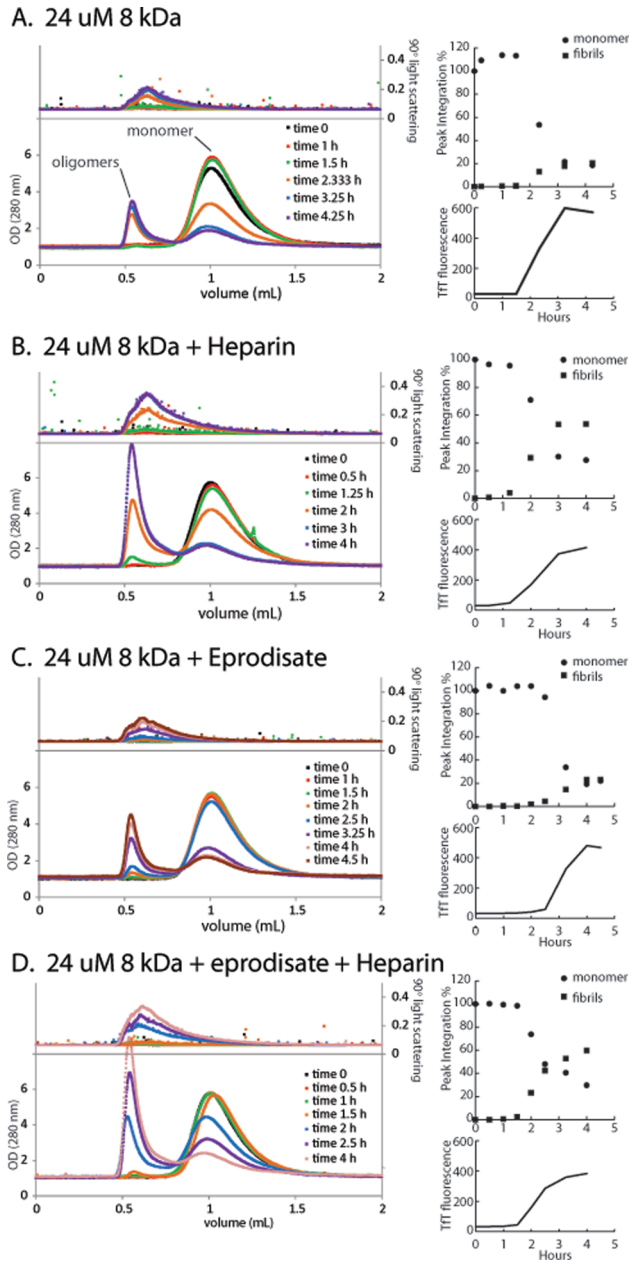

Figure 6. Analytical size exclusion chromatography (2 mL Superdex 75 column) of 8 kDa gelsolin amyloidogenesis reactions. For each experiment, an 8 kDa gelsolin amyloidogenesis reaction was performed in which 8 kDa gelsolin (24 μM) without GAGs or GAG mimetics (A), with heparin (10 μg/mL) (B), with eprodisate sodium (1 mM) (C), or with both heparin (10 μg/mL) and eprodisate (1 mM) (D) was mixed via overhead rotation (24 rpm) to form amyloid fibrils. At the indicated time points, an aliquot of the reaction mixture was examined by size exclusion chromatography, and 8 kDa gelsolin elution was detected by absorbance (280 nm), 90° static light scattering, and dynamic light scattering. The left panel of each set shows the overlaid absorption traces at the indicated time points (bottom) and overlaid 90° light scattering traces (top). Dynamic light scattering revealed the hydrodynamic radius of the oligomers eluting in the void volume to be between 60 and 80 nm. The far right panels depict the integration of the absorbance peaks at each time point (top) and the TfT fluorescence at each time point (bottom).

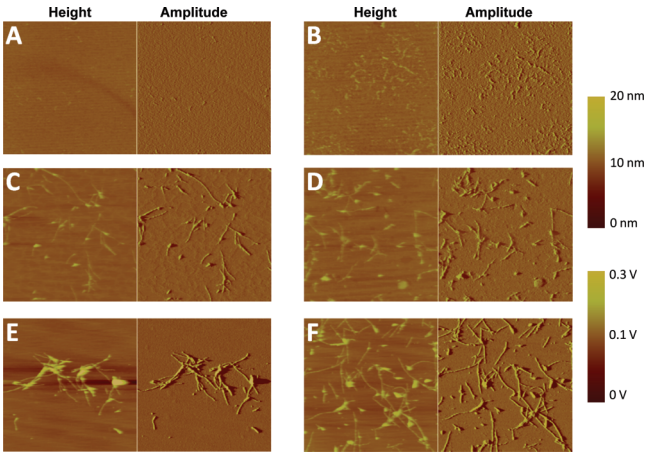

Figure 7. Representative tapping mode atomic force microscopy images of 8 kDa gelsolin amyloidogenesis reactions. The 8 kDa gelsolin (24 μM) was agitated via overhead rotation (24 rpm) in the absence (A, C, and E) or presence of heparin (10 μg/mL) (B, D, and F). Images were taken 40 (A), 100 (C), and 180 min (E) after the start of the amyloidogenesis reaction for the samples examined in the absence of heparin and 40 (B), 80 (D), and 180 min (F) after the start of the reaction for the samples examined in the presence of heparin (10 μg/mL). Thioflavin T fluorescence readings were taken at the same time as the samples were prepared for AFM analysis.

presence of eprodisate sodium in the reaction mixture with heparin also did not affect the solubility of the oligomers (cf. panel D to panel B of Figure 6). It therefore does not seem that GAG mimetics affect the solubility of oligomers to a great extent.

To determine if heparin had any effect on the morphology of the amyloid fibrils being formed, either early or in the late stages of the aggregation reaction, samples of 8 kDa gelsolin fibrils [24 μM, mixed via overhead rotation (24 rpm)] in the absence or presence of heparin (10 μg/mL) were examined by AFM and by TfT fluorescence as a function of time. In the absence of heparin, nothing could be observed by AFM after 40 min (Figure 7A) and the TfT signal was roughly equivalent to that of buffer, suggesting that there are no cross-β-sheet oligomers or fibrils. In the presence of heparin, however, a few small oligomers or protofibrils could be observed by AFM after 40 min (Figure 7B), when the TfT fluorescence had just begun to increase and was 2% of the maximum. As the aggregation time course continued, fibrils could be seen in the absence of heparin [Figure 7C (after 100 min), TfT fluorescence being 60% of the maximum] and in the presence of heparin [Figure 7D (after 80 min), TfT fluorescence being 55% of the maximum]. After 180 min, in the absence (Figure 7E) and presence of heparin (Figure 7F), the amyloid fibrils have continued to extend, and their further lateral association can be observed, more so in the absence of heparin. In general, however, heparin did not seem to cause an appreciable difference in amyloid fibril morphology.

Heparin Accelerates the Fibril Extension of the Amyloidogenesis Reaction and Reduces the Critical Concentration. The k_2 values obtained by fitting the 8 kDa gelsolin aggregation TfT fluorescence-monitored time courses to the Finke—Watzky model afford quantitative information about the fibril extension phase of the amyloidogenesis reaction, but the model is a simplified model of protein aggregation.[36] Because it was previously demonstrated that the 8 kDa fragment of gelsolin aggregates by a nucleated polymerization mechanism with off-pathway aggregation,[33] we further examined the heparin mechanism via the Powers and Powers model.[42,43] This model is characterized by a lag phase, during which a high-energy oligomer or nucleus is formed, after which amyloid fibrils are extended in a thermodynamically

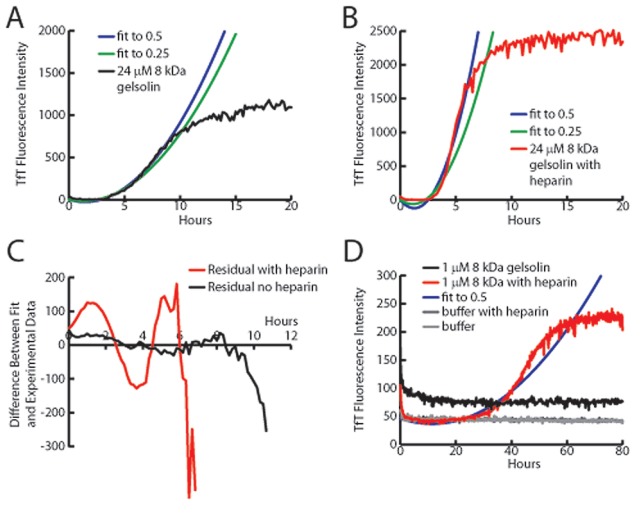

Figure 8. An 8 kDa gelsolin amyloidogenesis reaction (24 μM) in the absence (A) or presence (B) of heparin (10 μg/mL) was performed, and the data up to either 25 or 50% of the maximal TfT fluorescence were then fit to a second-degree polynomial (green curve or blue curve, respectively). (C) Residuals calculated as experimental data minus best fit curves. (D) Amyloidogenicity of 1 μM 8 kDa gelsolin examined in the absence (black) or presence (red) of heparin (10 μg/mL). The data for the 8 kDa gelsolin amyloidogenesis reaction up to 50% of the maximal fluorescence were then fit to a second-degree polynomial (blue).

favorable fibril extension reaction. In addition to the simple on-pathway fibril nucleus growth, off-pathway amorphous aggregates likely form. If the 8 kDa fragment of gelsolin aggregates by this mechanism, the lag and growth phases of the experimental data should fit to the equation

$$X = c_1 t^2 + c_2 t \qquad (2)$$

where X is the TfT fluorescence intensity.[42]

The fits of the data from a plate reader 8 kDa gelsolin aggregation assay (24 μM) in the absence of heparin up to 25 and 50% of the maximal fluorescence (Figure 8A, green and blue curves, respectively) fit almost equally well to the experimental data. On the other hand, when heparin is added, the fit up to 25% completion fits poorly to the rest of the time course (Figure 8B). Notably, the fibril extension phase of the reaction seems to be faster than expected from the fit to 25% completion. The plot of the residuals of the fits to 50% of the maximal fluorescence further emphasizes the fact that the fit to eq 2 is worse when heparin is added (Figure 8C).

The presence of heparin reduces the concentration of 8 kDa gelsolin necessary to form amyloid. When 1 μM 8 kDa gelsolin was examined in a plate reader amyloidogenesis reaction in the absence of heparin, the TfT fluorescence signal did not change over the 80 h time scale of the aggregation reaction (Figure 8D, black curve). However, an analogous reaction solution that contained heparin (10 μg/mL) was able to form TfT-positive species (Figure 8D, red curve), suggesting that cross-β-sheet oligomers can more efficiently build up to detectable levels in the presence of heparin. Even at this low 8 kDa gelsolin concentration, the experimental data in the presence of heparin deviated from the fit of the quadratic equation given above beyond 50% completion (Figure 8D).

Collectively, these observations suggest that the presence of heparin is able to decrease the concentration of an amyloidogenic peptide necessary for the accumulation of TfT-positive aggregates. In addition, heparin seems to increase the rate of the fibril extension phase of the aggregation reaction to be faster than in the absence of GAGs, an observation supported by the k_2 constants in the Finke−Watzky model. We hypothesize this is the case because heparin binds to 8 kDa gelsolin cross-β-sheet oligomers, increasing the efficiency by which they can convert to high-molecular mass amyloid fibrils, presumably as a consequence of oligomer concentration, alignment, and fusion.

DISCUSSION

The deposition of amyloid in mammals is strongly associated with several extracellular matrix components, including glycoproteins and GAGs. The distribution of these components in mammals creates different biological environments, which may affect the extent and tissue distribution of amyloid deposition. Understanding the interaction between GAGs and amyloidogenic peptides and the mechanism by which GAGs accelerate amyloidogenesis provides important mechanistic insights that help us think about new therapeutic strategies. Several mechanisms have been posited to explain how GAGs accelerate amyloidogenesis, and these mechanisms are not necessarily mutually exclusive. In fact, GAGs could exert different roles for distinct amyloidogenic peptides.

Some have suggested that GAGs are a "scaffold" to which monomeric amyloidogenic peptide or proteins can bind, enhancing amyloid fibril formation by increasing the local concentration and orienting the precursors to facilitate amyloid fibril formation.[44] Our finding that heparin does not alter the intrinsically disordered structure of gelsolin and that monomeric gelsolin does not bind to heparin seems to eliminate this as a possible mechanism whereby heparin accelerates the rate of gelsolin aggregation.

Alternatively, others have hypothesized that GAGs bind to small amorphous aggregates or cross-β-sheet oligomers leading to an accelerated conformational conversion to cross-β-sheet fibrils.[14] We have no evidence for the formation of unstructured prenucleus oligomers in the absence or presence of heparin. The isodichroic point observed in the far-UV CD experiments is fully consistent with a nucleated polymerization, whereby a very low concentration of prenucleus oligomers with alternative structures exists. The isodichroic point also strongly suggests a common postnucleus cross-β-sheet quaternary structure in the oligomers and in the fibrils. Such a mechanism is also consistent with the far-UV CD transition occurring concomitantly with the increase in TfT fluorescence intensity associated with cross-β-sheet quaternary structure or amyloid formation. Moreover, the appearance of aggregate species by AFM and the increase in TfT fluorescence intensity occur simultaneously. Finally, analytical size exclusion chromatography did not reveal significant oligomer formation until the TfT fluorescence also began to increase, in the presence or absence of heparin. Overall, the lack of prenucleus non-cross-β-sheet quaternary structural intermediates suggests that any off-pathway aggregate formation is so minor that it is undetectable at the concentrations used herein.

Our data favor the hypothesis that GAGs bind to already formed 8 kDa gelsolin cross-β-sheet amyloid-like oligomers, or protofibrils, as they are sometimes called, accelerating their growth into amyloid fibrils, while preventing fibril disassembly (Figure 9).[45] We show that heparin was able to bind to cross-β-sheet oligomers and/or amyloid fibrils of 8 kDa gelsolin, and that

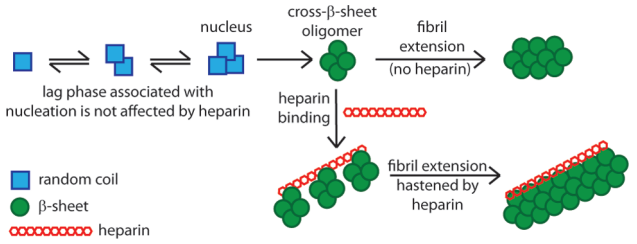

Figure 9. Mechanism for heparin acceleration of 8 kDa gelsolin amyloidogenesis that is consistent with all of the data described and presented here. Blue squares represent monomeric 8 kDa gelsolin adopting a random coil or non-β-sheet ensemble of structures. Green circles represent postnucleation 8 kDa gelsolin oligomers exhibiting a cross-β-sheet quaternary structure. The polymerized red hexagons represent heparin. Cross-β-sheet oligomers formed by a nucleated polymerization mechanism (not influenced by heparin) accumulate postnucleation and then bind to heparin, which subsequently accelerates the fibril extension phase of the amyloidogenesis reaction by binding, concentrating, aligning, and allowing the fusion of oligomers into amyloid fibrils.

the fibril extension phase of the amyloidogenesis reaction was accelerated by fitting our TfT fluorescence data to two different mathematical models of amyloidogenesis.

While the acceleration of fibril extension may occur by a few mechanisms, the most likely scenario involves concentrating and aligning oligomers and thus enhancing the frequency of oligomer fusion (Figure 9). Because monomeric 8 kDa gelsolin does not bind to heparin, it is unlikely that fibril extension is accelerated by enhanced recruitment of protein monomers. An increasing salt concentration dramatically reduces the effectiveness of heparin in accelerating the rate of amyloidogenesis, suggesting the importance of electrostatic interactions between the negatively charged heparin and the positively charged regions of gelsolin cross-β-sheet structure.

Some investigators have proposed that GAGs are key to causing amyloidogenesis and proteotoxicity in humans. Thus, substantial effort has been spent in the development of GAG mimetics, sulfonated small molecules that mimic the sulfated sugars of the extracellular matrix, to antagonize the GAG−amyloid interaction. These molecules were envisioned to antagonize the GAG-mediated acceleration of amyloidogenesis hypothesized to cause human amyloid diseases. These compounds have exhibited promise in clinical trials for the treatment of inflammation-associated amyloid disease, although the clinical trial results have not attained the expected clinical significance.[39−41] However, the GAG mimetics, eprosidate sodium and homotaurine, were not effective in inhibiting the heparin-mediated acceleration of 8 kDa gelsolin amyloidogenesis, nor did they affect the solubility of the oligomers. It therefore seems unlikely that sulfonated small molecules are able to generally antagonize the polyvalent effect of GAGs (Figure 9), which hastens the fibril extension phase of the amyloidogenesis reaction.

All of our data are consistent with the hypothesis that 8 kDa gelsolin aggregates by a nucleated polymerization mechanism in the absence or presence of heparin (Figure 9). In this mechanism, the random coil monomers very inefficiently form a high-energy oligomeric nucleus structure during the lag phase of the amyloidogenesis reaction, a step not influenced by the presence of heparin. The nucleus adds monomers and matures into a cross-β-sheet oligomer with kinetics that must be faster than those of nucleation, as the fibril extension phase of the aggregation dominates the TfT time course. Heparin appears to accelerate the growth phase of the aggregation reaction not by facilitating addition of the monomer to the cross-β-sheet oligomers (heparin does not bind the 8 kDa gelsolin monomer) but by binding and concentrating cross-β-sheet oligomers, apparently facilitating their fusion into higher-molecular mass cross-β-sheet structures, including amyloid fibrils, more efficiently than in the absence of heparin (Figure 9). The fact that the kinetics for the nucleated polymerization growth phase are faster than expected is consistent with this hypothesis. All evidence points only to the growth phase being accelerated by heparin. Lowering of the critical concentration of aggregation is most likely a consequence of fibril stabilization through heparin binding. It is possible that the reason that GAGs are upregulated in human amyloidoses and in amyloidosis animal models is that GAGs play a vital biological protective role by reducing proteotoxicity from small soluble cross-β-sheet oligomers by facilitating their fusion into fibrils that are rendered less proteotoxic through GAG-mediated fibril stabilization in the affected tissue. Such a protective mechanism is only effective in the GAG-stabilized amyloid deposits that do not displace key tissues.

■ ASSOCIATED CONTENT

Supporting Information. CD spectra of buffer and heparin controls (Figure 1), full 1D NMR spectra with water suppression of heparin, heparin with monomerized 8 kDa gelsolin, and heparin with 8 kDa gelsolin amyloid fibrils (Figure 2), amyloidogenesis reaction of 8 kDa gelsolin with fluorescein-labeled heparin (Figure 3), plate reader fluorescence polarization experiments (Figure 4), heparin affinity chromatography (Figure 5), gel mobility shift assay (Figure 6), raw data from plate reader amyloidogenicity assays showing each condition in triplicate (Figure 7), best fit Finke−Watzky curves for plate reader amyloidogenicity assay data (Figure 8), and analytical size exclusion chromatography (Figure 9). This material is available free of charge via the Internet at http://pubs.acs.org.

■ AUTHOR INFORMATION

Corresponding Author

*Phone: (858) 784-9605. Fax: (858) 784-9610. E-mail: jkelly@scripps.edu.

Funding Sources

This research was supported by National Institutes of Health Grant AG018917, the Skaggs Institute for Chemical Biology, and the Lita Annenberg Hazen Foundation.

■ ACKNOWLEDGMENT

We thank Colleen Fearns, Ji Young Suk, Lesley Page, and William E. Balch for helpful discussions and help with preparation of the manuscript, Gerard Kroon for help with the NMR experiments, and M. R. Ghadiri for use of his atomic force microscope.

■ ABBREVIATIONS

Aβ, amyloid β; AFM, atomic force microscopy; C68, C-terminal 68 kDa fragment of human plasma gelsolin; CD, circular dichroism; CNBr, cyanogen bromide; FAF, familial amyloidosis of

Finnish type; GAG, glycosaminoglycan; GdnHCl, guanidinium hydrochloride; MRE, mean residue ellipticity; MT1-MMP, membrane type 1 matrix metalloprotease; NaP_i, sodium phosphate; TfT, thioflavin T.

REFERENCES

(1) Gandhi, N. S., and Mancera, R. L. (2008) The structure of glycosaminoglycans and their interactions with proteins. *Chem. Biol. Drug Des. 72*, 455–482.

(2) Snow, A. D., Willmer, J., and Kisilevsky, R. (1987) Sulfated glycosaminoglycans: A common constituent of all amyloids. *Lab. Invest. 56*, 120–123.

(3) Young, I. D., Willmer, J. P., and Kisilevsky, R. (1989) The ultrastructural localization of sulfated proteoglycans is identical in the amyloids of Alzheimer's disease and AA, AL, senile cardiac and medullary carcinoma-associated amyloidosis. *Acta Neuropathol. 78*, 202–209.

(4) Alexandrescu, A. T. (2005) Amyloid accomplices and enforcers. *Protein Sci. 14*, 1–12.

(5) Ancsin, J. B. (2003) Amyloidogenesis: Historical and modern observations point to heparan sulfate proteoglycans as a major culprit. *Amyloid 10*, 67–79.

(6) Genedani, S., Agnati, L. F., Leo, G., Buzzega, D., Maccari, F., Carone, C., Andreoli, N., Filaferro, M., and Volpi, N. (2010) β-Amyloid fibrillation and/or hyperhomocysteinemia modify striatal patterns of hyaluronic acid and dermatan sulfate: Possible role in the pathogenesis of Alzheimer's disease. *Curr. Alzheimer Res. 7*, 150–157.

(7) Bergamaschini, L., Rossi, E., Storini, C., Pizzimenti, S., Distaso, M., Perego, C., De Luigi, A., Vergani, C., and De Simoni, M. G. (2004) Peripheral treatment with enoxaparin, a low molecular weight heparin, reduces plaques and β-amyloid accumulation in a mouse model of Alzheimer's disease. *J. Neurosci. 24*, 4181–4186.

(8) Timmer, N. M., Schirris, T. J. J., Bruinsma, I. B., Otte-Holler, I., van Kuppevelt, T. H., de Waal, R. M. W., and Verbeek, M. M. (2010) Aggregation and cytotoxic properties towards cultured cerebrovascular cells of Dutch-mutated Aβ40 (DAβ(1−40)) are modulated by sulfate moieties of heparin. *Neurosci. Res. 66*, 380–389.

(9) Perez, M., Wandosell, F., Colaco, C., and Avila, J. (1998) Sulphated glycosaminoglycans prevent the neurotoxicity of a human prion protein fragment. *Biochem. J. 335*, 369–374.

(10) Cortijo-Arellano, M., Ponce, J., Durany, N., and Cladera, J. (2008) Amyloidogenic properties of the prion protein fragment PrP-(185−208): Comparison with Alzheimer's peptide A β(1−28), influence of heparin and cell toxicity. *Biochem. Biophys. Res. Commun. 368*, 238–242.

(11) McLaurin, J., Franklin, T., Zhang, X. Q., Deng, J. P., and Fraser, P. E. (1999) Interactions of Alzheimer amyloid-β peptides with glycosaminoglycans: Effects on fibril nucleation and growth. *Eur. J. Biochem. 266*, 1101–1110.

(12) Yamaguchi, I., Suda, H., Tsuzuike, N., Seto, K., Seki, M., Yamaguchi, Y., Hasegawa, K., Takahashi, N., Yamamoto, S., Gejyo, F., and Naiki, H. (2003) Glycosaminoglycan and proteoglycan inhibit the depolymerization of β_2-microglobulin amyloid fibrils in vitro. *Kidney Int. 64*, 1080–1088.

(13) Relini, A., De Stefano, S., Torrassa, S., Cavalleri, O., Rolandi, R., Gliozzi, A., Giorgetti, S., Raimondi, S., Marchese, L., Verga, L., Rossi, A., Stoppini, M., and Bellotti, V. (2008) Heparin strongly enhances the formation of β_2-microglobulin amyloid fibrils in the presence of type I collagen. *J. Biol. Chem. 283*, 4912–4920.

(14) Bourgault, S., Solomon, J. P., Reixach, N., and Kelly, J. W. (2011) Sulfated glycosaminoglycans accelerate transthyretin amyloidogenesis by quaternary structural conversion. *Biochemistry 50*, 1001–1015.

(15) Suk, J. Y., Zhang, F. M., Balch, W. E., Linhardt, R. J., and Kelly, J. W. (2006) Heparin accelerates gelsolin amyloidogenesis. *Biochemistry 45*, 2234–2242.

(16) Maury, C. P. J. (1991) Gelsolin-related amyloidosis: Identification of the amyloid protein in Finnish hereditary amyloidosis as a fragment of variant gelsolin. *J. Clin. Invest. 87*, 1195–1199.

(17) Burtnick, L. D., Koepf, E. K., Grimes, J., Jones, E. Y., Stuart, D. I., Mclaughlin, P. J., and Robinson, R. C. (1997) The crystal structure of plasma gelsolin: Implications for actin severing, capping, and nucleation. *Cell 90*, 661–670.

(18) Sun, H. Q., Yamamoto, M., Mejillano, M., and Yin, H. L. (1999) Gelsolin, a multifunctional actin regulatory protein. *J. Biol. Chem. 274*, 33179–33182.

(19) DiNubile, M. J. (2008) Plasma gelsolin as a biomarker of inflammation. *Arthritis Res. Ther. 10*, 124.

(20) Lee, P. S., Sampath, K., Karumanchi, S. A., Tamez, H., Bhan, I., Isakova, T., Gutierrez, O. M., Wolf, M., Chang, Y. C., Stossel, T. P., and Thadhani, R. (2009) Plasma gelsolin and circulating actin correlate with hemodialysis mortality. *J. Am. Soc. Nephrol. 20*, 1140–1148.

(21) Kwiatkowski, D. J., Mehl, R., Izumo, S., Nadalginard, B., and Yin, H. L. (1988) Muscle is the major source of plasma gelsolin. *J. Biol. Chem. 263*, 8239–8243.

(22) Kazmirski, S. L., Isaacson, R. L., An, C., Buckle, A., Johnson, C. M., Daggett, V., and Fersht, A. R. (2002) Loss of a metal-binding site in gelsolin leads to familial amyloidosis-Finnish type. *Nat. Struct. Biol. 9*, 112–116.

(23) Huff, M. E., Page, L. J., Balch, W. E., and Kelly, J. W. (2003) Gelsolin domain 2 Ca^{2+} affinity determines susceptibility to furin proteolysis and familial amyloidosis of Finnish type. *J. Mol. Biol. 334*, 119–127.

(24) Chen, C. D., Huff, M. E., Matteson, J., Page, L. J., Phillips, R., Kelly, J. W., and Balch, W. E. (2001) Furin initiates gelsolin familial amyloidosis in the Golgi through a defect in Ca^{2+} stabilization. *EMBO J. 20*, 6277–6287.

(25) Kangas, H., Seidan, N. G., and Paunio, D. (2002) Role of proprotein convertases in the pathogenic processing of the amyloidosis-associated form of secretory gelsolin. *Amyloid 9*, 83–87.

(26) Nag, S., Ma, Q., Wang, H., Chumnarnsilpa, S., Lee, W. L., Larsson, M., Kannan, B., Hernandez-Valladarez, M., Burtnick, L. D., and Robinson, R. C. (2009) Ca^{2+} binding by domain 2 plays a critical role in the activation and stabilization of gelsolin. *Proc. Natl. Acad. Sci. U.S.A. 106*, 13713–13718.

(27) Page, L. J., Suk, J. Y., Huff, M. E., Lim, H. J., Venable, J., Yates, J., Kelly, J. W., and Balch, W. E. (2005) Metalloendoprotease cleavage triggers gelsolin amyloidogenesis. *EMBO J. 24*, 4124–4132.

(28) Kiuru-Enari, S., Keski-Oja, J., and Haltia, M. (2005) Cutis laxa in hereditary gelsolin amyloidosis. *Br. J. Dermatol. 152*, 250–257.

(29) Kiuru, S., Matikainen, E., Kupari, M., Haltia, M., and Palo, J. (1994) Autonomic nervous system and cardiac involvement in familial amyloidosis, Finnish type (FAF). *J. Neurol. Sci. 126*, 40–48.

(30) Kivela, T., Tarkkanen, A., Frangione, B., Ghiso, J., and Haltia, M. (1994) Ocular amyloid deposition in familial amyloidosis, Finnish: An analysis of native and variant gelsolin in Meretojas syndrome. *Invest. Ophthalmol. Visual Sci. 35*, 3759–3769.

(31) Kiuru-Enari, S., Somer, H., Seppalainen, A. M., Notkola, I. L., and Haltia, M. (2002) Neuromuscular pathology in hereditary gelsolin amyloidosis. *J. Neuropathol. Exp. Neurol. 61*, 565–571.

(32) Page, L. J., Suk, J. Y., Bazhenova, L., Fleming, S. M., Wood, M., Jiang, Y., Guo, L. T., Mizisin, A. P., Kisilevsky, R., Shelton, G. D., Balch, W. E., and Kelly, J. W. (2009) Secretion of amyloidogenic gelsolin progressively compromises protein homeostasis leading to the intracellular aggregation of proteins. *Proc. Natl. Acad. Sci. U.S.A. 106*, 11125–11130.

(33) Solomon, J. P., Yonemoto, I. T., Murray, A. N., Price, J., Powers, E. T., Balch, W. E., and Kelly, J. W. (2009) The 8 and 5 kDa fragments of plasma gelsolin form amyloid fibrils by a nucleated polymerization mechanism, while the 68 kDa fragment is not amyloidogenic. *Biochemistry 48*, 11370–11380.

(34) Yonemoto, I. T., Wood, M. R., Balch, W. E., and Kelly, J. W. (2009) A general strategy for the bacterial expression of amyloidogenic peptides using BCL-XL-1/2 fusions. *Protein Sci. 18*, 1978–1986.

(35) Glabe, C. G., Harty, P. K., and Rosen, S. D. (1983) Preparation and properties of fluorescent polysaccharides. *Anal. Biochem. 130*, 287–294.

(36) Morris, A. M., Watzky, M. A., Agar, J. N., and Finke, R. G. (2008) Fitting neurological protein aggregation kinetic data via a 2-step, Minimal/"Ockham's Razor" model: The Finke-Watzky mechanism of nucleation followed by autocatalytic surface growth. *Biochemistry 47*, 2413–2427.

(37) Seo, E. S., Blaum, B. S., Vargues, T., De Cecco, M., Deakin, J. A., Lyon, M., Barran, P. E., Campopiano, D. J., and Uhrin, D. (2010) Interaction of human β-defensin 2 (HBD2) with glycosaminoglycans. *Biochemistry 49*, 10486–10495.

(38) Hawe, A., Sutter, M., and Jiskoot, W. (2008) Extrinsic fluorescent dyes as tools for protein characterization. *Pharm. Res. 25*, 1487–1499.

(39) Dember, L. M., Hawkins, P. N., Hazenberg, B. P. C., Gorevic, P. D., Merlini, G., Butrimiene, I., Livneh, A., Lesnyak, O., Puechal, X., Lachmann, H. J., Obici, L., Balshaw, R., Garceau, D., Hauck, W., Skinner, M., and Eprodisate for AA Amyloidosis Trial Group. (2007) Eprodisate for the treatment of renal disease in AA amyloidosis. *N. Engl. J. Med. 356*, 2349–2360.

(40) Kisilevsky, R., Ancsin, J. B., Szarek, W., and Petanceska, S. (2007) Heparan sulfate as a therapeutic target in amyloidogenesis: Prospects and possible complications. *Amyloid 14*, 21–32.

(41) Kisilevsky, R., Lemieux, L. J., Fraser, P. E., Kong, X. Q., Hultin, P. G., and Szarek, W. A. (1995) Arresting amyloidosis in vivo using small-molecule anionic sulphonates or sulphates: Implications for Alzheimer's disease. *Nat. Med. 1*, 143–148.

(42) Powers, E. T., and Powers, D. L. (2008) Mechanisms of protein fibril formation: Nucleated polymerization with competing off-pathway aggregation. *Biophys. J. 94*, 379–391.

(43) Ferrone, F. A. (1999) Analysis of protein aggregation kinetics. *Methods Enzymol.* 309, 256−274.

(44) Motamedi-Shad, N., Monsellier, E., Torrassa, S., Relini, A., and Chiti, F. (2009) Kinetic analysis of amyloid formation in the presence of heparan sulfate: Faster unfolding and change of pathway. *J. Biol. Chem. 284*, 29921–29934.

(45) Watson, D. J., Lander, A. D., and Selkoe, D. J. (1997) Heparin-binding properties of the amyloidogenic peptides Aβ and amylin: Dependence on aggregation state and inhibition by Congo red. *J. Biol. Chem. 272*, 31617–31624.